Since the experimental data in the neighborhood of $\hat{H}\|\hat{q}$ are in satisfactory agreement with the theory given here, there is no experimental evidence of the parallel field effect suggested by Daniel and Mackinnon.

We should like to comment upon the application of this effect to the study of band structure. If the magnetic field is parallel to the sound wave vector, then we measure the linear dimension of the orbit parallel to the magnetic field. However, this gives no *direct* information about the orbit in p space, because, as known, $\mathbf{p}(t)=(e/c)[\mathbf{r}(t)\times\mathbf{H}]$. Thus, that part of the orbit in real space which is parallel to the magnetic field does not contribute to the p-space orbit at all. However, if a model of the Fermi surface is already known, then the equations of motion may be solved to find the orbit in real space, as was done for the ellipsoidal case, and additional information regarding the Fermi surface will be obtained. The parallel field effect might also find application in singling out those sheets of the Fermi surface which are tilted with respect to a symmetry axis. For example, if $\hat{q}\|\hat{H}\|[001]$ axis of tin, only four of a possible ten sheets predicted by the free electron model of the Fermi surface would contribute to geometric resonances.[8]

[8] A. V. Gold and M. G. Priestley, Phil. Mag. **5**, 1089 (1960).

PHYSICAL REVIEW VOLUME 135, NUMBER 3A 3 AUGUST 1964

Infrared Lattice Vibrations in Calcium Tungstate and Calcium Molybdate

A. S. Barker, Jr.
Bell Telephone Laboratories, Murray Hill, New Jersey
(Received 9 March 1964)

The infrared active lattice vibrations of single-crystal $CaWO_4$ and $CaMoO_4$ have been studied by taking polarized reflection spectra in the region 1 to 130 μ. Four infrared phonon modes vibrate with the electric vector E parallel to the c axis and four with E perpendicular to the c axis in each material. A classical oscillator dispersion analysis is carried out to give the mode strengths, frequencies, and linewidths of the eight infrared modes. The frequencies of the eight corresponding longitudinal optic modes are found from the dispersion analysis. A symmetry study of the zero wave vector vibrations is carried out for the Scheelite structure which predicts four infrared modes for $E\|c$ axis and four for $E\perp c$ axis as well as 13 Raman modes and 3 inactive modes. A study is made of apparent failure of the classical oscillator model near one of the strong modes.

INTRODUCTION

LARGE single crystals of calcium tungstate and molybdate have recently become available as a result of perfection of the Czochralski growth method for oxide systems.[1,2] These crystals can be readily doped with rare-earth ions during growth. The doped crystals are the subject of much current optical maser study.[3,4] This paper describes measurements of the infrared reflectivity for the pure materials. Very little has been done since Coblentz's infrared work on $CaWO_4$ in 1908.[5] In that work one restrahlen band was reported near 12 μ for an unoriented sample. In the present work eight infrared allowed modes are seen in the reflection spectra. A dispersion analysis is carried out which yields the strengths, resonant frequencies, and linewidths of the infrared-active phonon modes and the frequencies of the associated longitudinal optic modes. The results are shown to be in agreement with a study made of the group character table for the Scheelite structure.

[1] K. Nassau and A. M. Broyer, J. Appl. Phys. **33**, 3064 (1962).
[2] S. Preziosi, R. R. Soden, and L. G. Van Uitert, J. Appl. Phys. **33**, 1893 (1962).
[3] L. F. Johnson, J. Appl. Phys. **34**, 897 (1963). L. F. Johnson and R. A. Thomas, Phys. Rev. **131**, 2038 (1963).
[4] L. F. Johnson, L. G. Van Uitert, J. J. Rubin, and R. A. Thomas, Phys. Rev. **133**, A494 (1964).
[5] W. Coblentz, *Supplementary Investigations of Infrared Spectra* (The Carnegie Institution, Washington, 1908), Publication No. 97, p. 16.

EXPERIMENTAL

Boules of undoped $CaWO_4$ and $CaMoO_4$ were obtained and oriented by x ray. Two slabs about 1 by 1 by 0.4 cm were then cut from each boule. The slabs were cut so that the large face was perpendicular to the c axis in one sample and perpendicular to the a axis in the other. The faces and some edges were then polished. Both materials are quite soft. Satisfactory results were obtained by progressing from 400 grit sandpaper to Buehler M305 abrasive then directly to Linde-A polishing compound using water slurrys on plate glass laps. After polishing the samples, the c axis could be located quite easily from the optic figure seen with crossed polaroids.

Room-temperature polarized reflection spectra were taken for the electric vector E parallel to the c axis and then for E parallel to an a axis. This choice selects the major and minor axes of the dielectric ellipsoid and will thus specify the complete optic behavior when the reflection spectra are suitably analyzed. The measure-

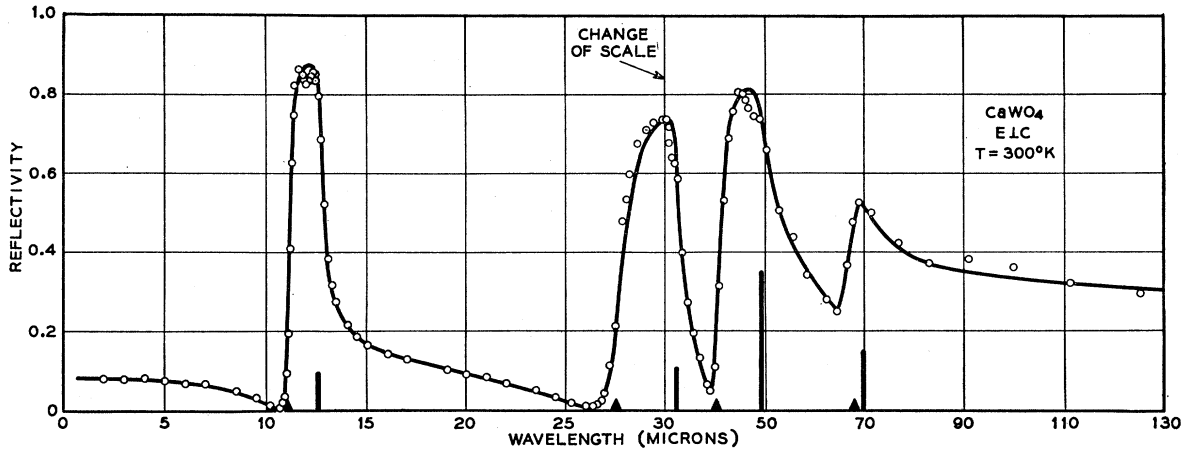

FIG. 1. Reflectivity of calcium tungstate for the electric vector perpendicular to the c axis. The curve shows the best fit obtained with the classical oscillator dispersion formula. In this and succeeding figures the dark vertical bars give the infrared (transverse) mode strengths and frequencies (a height of 0.1 is a strength of 1.0) and the triangles give the frequencies of the longitudinal modes.

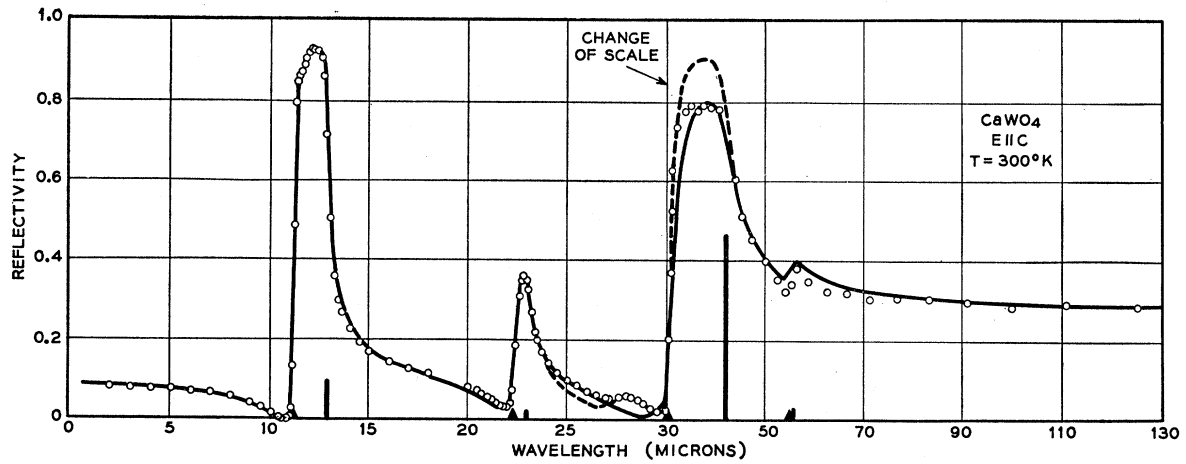

FIG. 2. Reflectivity of calcium tungstate for the electric vector parallel to the c axis. The solid curve gives the best classical oscillator fit in the sense described in the text. The dashed curve is an alternate fit.

ments were made through the wavelength region 1–130 μ. A double-pass prism spectrometer was used from 1–35 μ and a single-pass grating spectrometer from 30–130 μ. In the 1–35-μ region, spectra were run on at least two different samples of each material. The spectra from different samples agreed well except for one sample of $CaMoO_4$. This $CaMoO_4$ sample exhibited restrahlen peaks at the correct frequencies but the peaks had anomalously low reflectivities. This sample was not studied further and is not presented here. In the long-wavelength region an anomalous flat-topped restrahlen peak was encountered in $CaWO_4$ ($E\|C$). This peak was found to be identical (within 2%) in the two samples studied and is discussed in considerable detail in a later section. The reflectivity near a restrahlen peak is known to be sensitive to surface condition of the sample for some materials.[6,7] It has been found that chemical etching can raise the maximum reflectivity and restore the spectral shape to that predicted by a simple oscillator.[6,7] To test whether surface damage arising from mechanical polishing is responsible for the unusual spectral shape encountered in $CaWO_4$, one sample was chemically polished to remove at least 5 μ from the surface then rerun in the region 240–320 cm^{-1} ($E\|C$). The reflectivity remained unchanged within 1.5%. There was no consistent shift to higher reflectivity, the 1.5% is about the reproducibility figure arising from noise and sample mounting procedure. For all spectra, the reflectivity was measured at an angle of incidence of about 15°. The general method of making the measurements has been described previously by others.[8]

Figures 1 through 4 show the measured reflectivity. We note four modes for each polarization in both mate-

[6] D. A. Kleinman and W. G. Spitzer, Phys. Rev. **118**, 110 (1960).
[7] A. S. Barker, Jr., Phys. Rev. **132**, 1474 (1963).
[8] W. G. Spitzer and D. A. Kleinman, Phys. Rev. **121**, 1324 (1961).

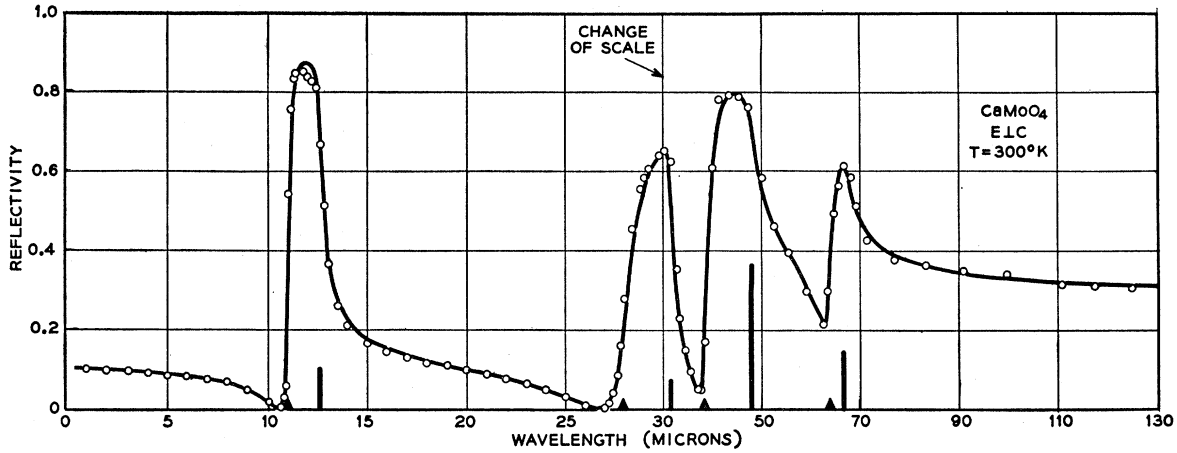

FIG. 3. Reflectivity of calcium molybdate for the electric vector perpendicular to the c axis. The solid curve shows the best classical oscillator fit.

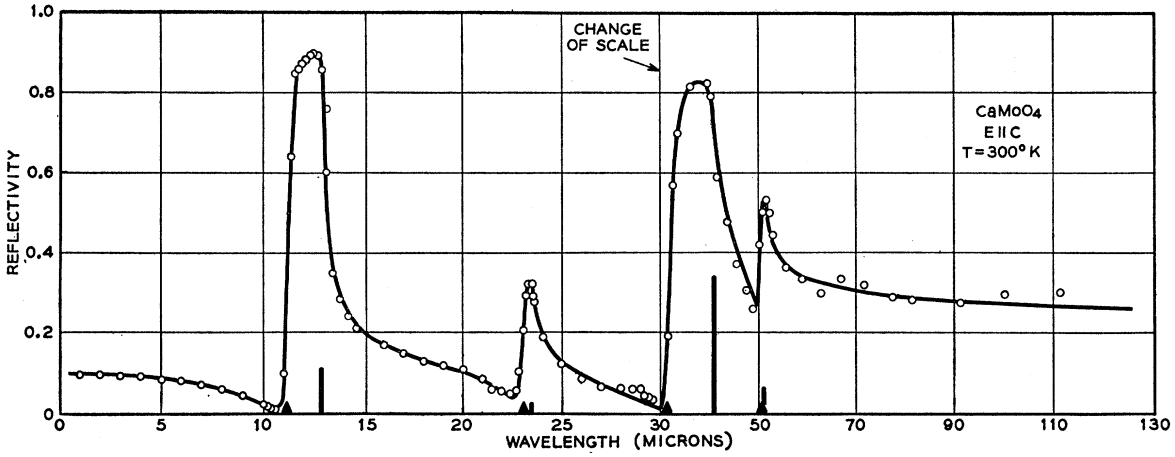

FIG. 4. Reflectivity of calcium molybdate for the electric vector parallel to the c axis. The solid curve is the best classical oscillator fit.

rials. The solid curves are the result of fits using the dispersion theory which is described below.

ANALYSIS

The measured reflectivity R of a material may be complimented by an analysis which yields the optical constants n and k or ϵ' and ϵ''. The two procedures commonly used are the Kramers-Kronig inversion of R and the fitting of the classical oscillator formula to R,[8] while the first method may in theory give exactly ϵ' and ϵ'', independent of any model, in practice the method suffers from inaccuracy when $\epsilon'' \ll \epsilon'$. In the present work the second method was used, though a Kramers-Kronig transform was used on some of the spectra to establish initially the linewidths and strengths of the modes.

The classical oscillator formula for the complex dielectric constant is

$$\epsilon(\omega)=\epsilon'-i\epsilon''=\sum_j \frac{S_j\omega_j^2}{\omega_j^2-\omega^2+i\omega\gamma_j}+\epsilon_\infty, \qquad (1)$$

where S_j, ω_j, γ_j are the strength, resonant frequency, and linewidth, respectively, of the jth mode. ϵ_∞ gives the asymptotic behavior for very high frequencies and can usually be estimated with sufficient accuracy from the reflectivity near 1–3-μ wavelength. The procedure consists of assigning values to S_j, ω_j, γ_j, ϵ_∞ then calculating the reflectivity R. Changes are made in the assignments to improve the fit of this calculated R to the measured points. This whole procedure is carried out separately for the two polarizations, $E\perp c$ axis and $E\|c$ axis. The fitting in the present work was done using the full Fresnel formula for R to allow for the angle of incidence used in the experiments. The main effect of taking proper account of the angle of incidence is changes by a few percent in ϵ_∞ and in the mode linewidths, from what would be predicted using the normal incidence Fresnel formula. The effect is important only for certain modes whose linewidths can be determined to better than 10% accuracy. The solid lines in Figs. 1–4 show the best fits obtained using Eq. (1) and the

TABLE I. Classical oscillator dispersion parameters for $CaWO_4$. l designates longitudinal modes and f forbidden modes. The alternate fit described in the test (dashed curve in Figs. 2 and 7) for $E\|c$ was obtained by adding the mode f^* and substituting the bracketed values where indicated.

	$\lambda_i(\mu)$	$\omega_i(\text{cm}^{-1})$	Si	γ_i/ω_i
		$E\perp c$		
	69.8	143	1.5	0.07
	49.5	202	3.5	0.05
	32.4	309	1.06	0.038
	12.6	793	0.93	0.012
l	68.0	147.5		
l	40.3	248		
l	27.5	363	$\epsilon_\infty=3.4$[a]	
l	11.4	905		
f	100	100	$\epsilon_\infty+\sum_i S_i=10.4$	
f	47	213		
f	31	322		
f	11.9	840		
f	11.2	893		
		$E\|c$		
	55.6	180	0.3	0.06
	42.2 (41.7)	237 (240)	4.65	0.075 (0.03)
	23.0	435	0.22	0.026
	12.85	778	0.97	0.007
f^*	27.8	360	0.1	0.1
l	55.0	182		
l	30.5	327	$\epsilon_\infty=3.5$[a]	
l	22.3	448		
l	11.2	893	$\epsilon_\infty+\sum_i S_i=9.7$	
f	36.4 (uncertain)	275		
f	11.8	850.0		

[a] The indices of refraction at 0.59 microns given in the *Handbook of Chemistry and Physics* (Chemical Rubber Company, Cleveland, 1959) would predict an ϵ_∞ ten percent higher than reported here. Recent measurements by W. L. Bond (private communication), however, show considerable dispersion of the index of refraction between 2.0 and 0.59 μ.

procedure described above. Typically the frequency of a mode is determined to better than 1%, the strength to 5 to 10% and the linewidth to better than 15% by the fitting process. The modes are represented in each figure by short vertical bars whose height is proportional to the mode strength. In addition, the longitudinal optic mode frequencies may be obtained by noting the frequency where Real $(\epsilon)=0$. These frequencies are also shown in the figures. Tables I and II list the mode parameters used to obtain the theoretical reflectivity curves, and other quantities of interest.

Group Character Analysis

$CaWO_4$ and $CaMoO_4$ crystallize in the Scheelite structure which has space group I_{4_1}/a. The unit cell is usually taken to be body centered tetragonal with two formula units associated with each lattice point. One must carefully select the primitive cell before beginning the group character analysis. Lax has given transformation formulas relating the primitive cell axes to the conventional cell axes.[9]

The primitive cell is shown in Fig. 5 along with the conventional cell. The point group is C_{4h}. Table III

[9] M. Lax, *Symmetry Principles in Solid State Physics* (to be published).

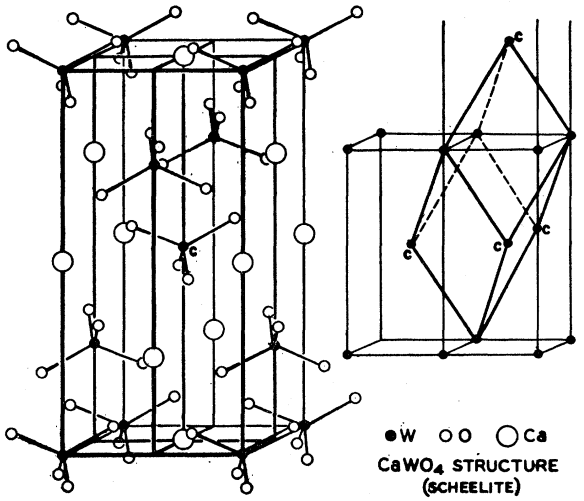

FIG. 5. Conventional body-centered-tetragonal cell of calcium tungstate showing the ion positions. This cell contains four formula units. To the right is shown the primitive cell (two formula units) and its relation to the tetragonal cell. The centered position of the tetragonal cell has been marked c.

shows the appropriate character table. The character for a general displacement of all atoms in the cell has been constructed and listed along the bottom row of the table. This general displacement must be made up of a linear combination of the symmetry mode displacements (which transform according to the irreducible representations). The resolution of the general displacement into irreducible representations has been carried out with the result shown in the right-hand columns in Table III. We are most directly interested in irreducible

TABLE II. Classical oscillator dispersion parameters for $CaMoO_4$. l designates longitudinal modes and f forbidden modes.

	$\lambda_i(\mu)$	$\omega_i(\text{cm}^{-1})$	Si	γ_i/ω_i
		$E\perp c$		
	66.7	150	1.5	0.042
	48.1	208	3.7	0.060
	31.4	318	0.80	0.040
	12.5	802	0.96	0.012
l	64.0	156		
l	38.3	261	$\epsilon_\infty=3.8$[a]	
l	27.9	358		
l	10.96	913	$\epsilon_\infty+\sum_i S_i=10.8$	
f	11.2	893		
		$E\|c$		
	51.0	196	0.6	0.025
	40.8	245	3.4	0.050
	23.5	425	0.2	0.026
	12.9	775	1.1	0.011
l	50.7	197		
l	31.4	319	$\epsilon_\infty=3.7$[a]	
l	23.0	434	$\epsilon_\infty+\sum_i S_i=9.0$	
l	11.4	897		
f	29	345		
f	21 (uncertain)	476		
f	11.6	862		

[a] The indices of refraction at 0.59 μ (see Ref. a of Table I) predict an ϵ_∞ of about 3.8 for both axes.

TABLE III. Character table, symmetry modes, and selection rules for Scheelite.

Space group $I4_1/a$		Point group (C_{4h}) operations E	C_2	C_4	C_4^3	i	iC_2	iC_4	iC_4^3	Number of irred reps in general Cartesian rep	Modes at $k=0$ Acoustic	Optic	Sel. rule
Irreducible representations of the point group C_{4h}	Ag	1	1	1	1	1	1	1	1	3		3	R
	Bg	1	1	−1	−1	1	1	−1	−1	5		5	R
	Eg	1	−1	i	$-i$	1	−1	i	$-i$	5		5	R
		1	−1	$-i$	i	1	−1	$-i$	i	0			
	Au	1	1	1	1	−1	−1	−1	−1	5	1	4	IR ($E\|C$)
	Bu	1	1	−1	−1	−1	−1	1	1	3		3	
	Eu	1	−1	i	$-i$	−1	1	$-i$	i	5	1	4	IR ($E\perp C$)
		1	−1	$-i$	i	−1	1	i	$-i$	0			
Representation of the general Cartesian displacement of all atoms		36	−4	0	0	0	0	−4	−4	Selection rules R=allowed Raman transition IR=allowed infrared transition			

representations Au and Eu since ion motions which generate dipole moment along the c axis and perpendicular to the c axis, respectively, must come under these representations.[10,11] For these two representations we subtract off the one translational mode of motion (Acoustic mode). We find there are four infrared active modes with the electric vector E parallel to the c axis, and four perpendicular to the c axis. Modes which are Raman active are also noted in the table. In addition to the Raman active and infrared active modes, there are three optic modes which are inactive.

DISCUSSION

The classical oscillator analysis of the tungstate and molybdate reflectivity data has yielded the four modes for each polarization in agreement with the group character analysis. The reflectivity fit is not as good as has been achieved with some other materials. The fit could be improved in some regions by adding extra weaker modes, for example, near 28 and 36 μ for $CaWO_4$ ($E\|C$). Such modes can arise from selection rule breakdown in infrared inactive vibration[7] or from multiphonon absorption (combination bands). We will call all such extra weak modes forbidden modes. The forbidden mode at 27.8 μ in $CaWO_4$ ($E\|C$) was studied by fitting the reflectivity carefully in this region. The strength, frequency and linewidth parameters are given in Table I. Other forbidden modes appeared much weaker and no attempt was made to fit them.

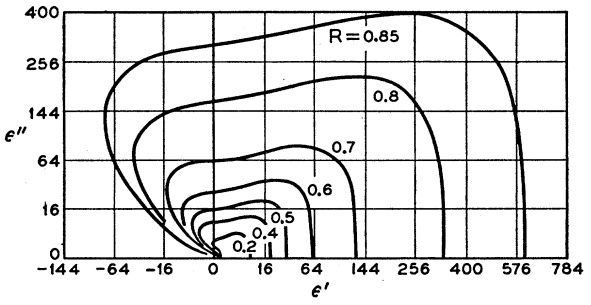

FIG. 6. Normal incidence reflectivity as a function of the real and imaginary parts of the dielectric constant ϵ' and ϵ''.

In $CaWO_4$ ($E\|C$) the wavelength region 30 to 70 μ proved very difficult to fit with the classical formulas. The strongest mode encountered in the study appears in this range fairly close to one of the weakest modes and to the strong "extra" or forbidden mode described above. This region was studied in some detail using Kramers-Kronig analysis and many different classical oscillator fits. Two points arose from this study which probably are worth emphasizing. First, the reflectivity is in general quite insensitive to ϵ'' on the long wavelength side of a mode. On passing to wavelengths below the mode resonance ϵ' goes through a dispersion and becomes negative. With ϵ' negative the reflectivity is now quite sensitive to ϵ'' even where it is much smaller than ϵ'. Figure 6 shows the reason for this behavior. The figure gives reflectivity as a function of ϵ' and ϵ''. For ϵ' positive and greater than ϵ'' the lines of constant reflectivity are nearly vertical (i.e., independent of ϵ''), while for ϵ' negative, ϵ' and ϵ'' are equally important in determining the reflectivity.

The second point to be made is that far from an infrared resonance, the classical form for ϵ' should be quite good. The Kramers-Kronig relation between ϵ' and ϵ'' can be used to show this. If the mode in ϵ'' is fairly well peaked only the area under its curve, not the details of its shape, determines ϵ' at frequencies far from the mode.

Combining the above arguments, we see we can always expect a good classical oscillator fit to *reflectivity* on the long wavelength side of a mode. The real test of classical oscillator behavior is the reflectivity fit between the infrared or transverse frequency ω_t and the longitudinal frequency ω_l which is the region where ϵ' is negative. These points were not appreciated when the first fits were attempted. Since the very strong mode in

[10] M. Tinkham, *Group Theory and Quantum Mechanics* (McGraw-Hill Book Company, Inc., New York, 1964), Chap. 7.
[11] S. Bhagavantam and T. Venkatarayudu, Proc. Indian Acad. Sci. **9A**, 224 (1939).

$CaWO_4$ (Fig. 2) has an anomalous flat top, it was tempting to ignore the fit along the top and concentrate on the steep edges of the restrahlen band. The result of this first fit is the dashed curve shown in Fig. 2. (Table I gives the mode parameters.) The fit shown by the solid curve was made next by trying to fit the reflectivity at frequencies below the mode resonant frequency and doing the best possible job of fitting about midway between ω_t and ω_l, i.e., around 37 μ. The poor fit from about 27 to 34.5 μ was ignored. Also the forbidden mode at 360 cm^{-1} was not included in this fit.

We may now compare these two classical oscillator fits with the actual behavior of ϵ'' obtained from a Kramers-Kronig analysis. In Fig. 7 ϵ'' from the first fit is again shown as a dashed curve and what we regard as the best fit is shown by the solid curve. The points were obtained from the Kramers-Kronig analysis of the reflectivity. We note that we were completely misled in the first fit (dashed) by attaching so much importance to the steep short wavelength side of restrahlen band. The details of ϵ'' which it is our aim to establish are given much more accurately by the solid curve fit which in some respects looks worse in reflectivity.

The graph of ϵ'' discussed above serves as a basis for discussing other features of the reflectivity fit in the region 30 to 70 μ for $CaWO_4$ ($E\|C$). We note that ϵ'' given by the Kramers-Kronig analysis dips below classical oscillator values given by the solid curve. This situation has been encountered in the perovskites where the dip in ϵ'' between modes was very pronounced and dominated the reflectivity in a much stronger way than here.[12,13] With the perovskites a mode interaction theory has been developed which can account for such low absorption between modes.[13] In this theory, for a pair of modes there are the usual six parameters (strength, frequency, and linewidth for each mode) plus an interaction damping parameter which has as its main effect the increase or reduction of ϵ'' between the modes. The effect will be largest near a strong mode. A comparison with the perovskite results[13] indicates that the steep reflectivity rise at 31 μ (Fig. 2) is to be associated with the dip in ϵ'' near 31 μ and thus will not be given by the classical oscillator fit used here. Similarly, in $CaWO_4$ ($E\perp c$) the failure of the ordinary classical model to reproduce the steep rise in reflectivity near 29 μ may be a sign of interaction damping. The reason for the poor fit near 56 μ in $CaWO_4$ ($E\|C$) is not understood. We note from Fig. 7, however, that the classical oscillator strength, frequency and linewidth for the 56-μ mode do provide a reasonable picture of the mode structure.

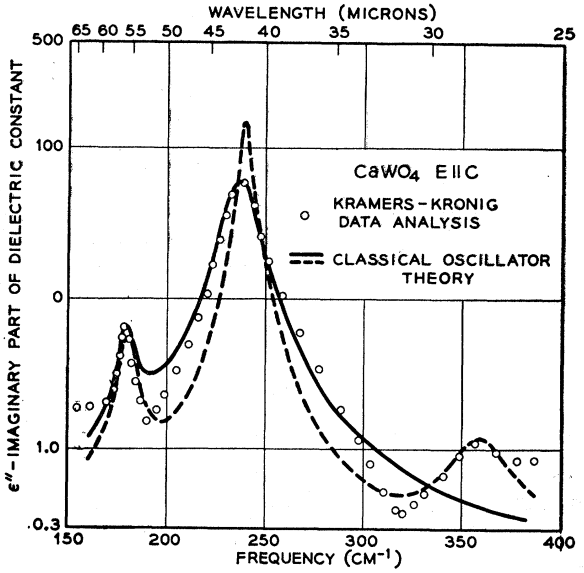

FIG. 7. Imaginary part of the dielectric constant of calcium tungstate for the electric vector parallel to the c axis. The points were obtained directly from the reflectivity data using a Kramers-Kronig integral transform. The solid curve results from what we have called the "best" classical oscillator fit to reflectivity. The dashed curve is an alternate fit which gives a different reflectivity in the region of interest 200–300 cm^{-1}. In addition the alternate fit includes a forbidden mode at 360 cm^{-1}.

To summarize, fitting the reflectivity in a suitable way with the classical oscillator formula has yielded the frequencies, strengths and linewidths of the infrared modes. One forbidden mode in $CaWO_4$ has also been characterized by a strength frequency and linewidth. A similar forbidden mode appears in $CaMoO_4$ which has a shifted frequency but much the same strength and linewidth. The frequencies of other forbidden modes are listed in Tables I and II. Some of these latter modes are too narrow or shallow to show in Figs. 1–4. The Kramers-Kronig study coupled with the classical oscillator fitting has shown that the region of maximum reflectivity (*restrahlen* band) must be fit carefully even at the expense of a poor fit elsewhere to obtain meaningful mode parameters.

ACKNOWLEDGMENTS

It is a pleasure to acknowledge the cooperation of K. Nassau and J. Rubin for supplying the samples and A. Contaldo for taking a number of the infrared spectra.

[12] W. G. Spitzer, R. C. Miller, D. A. Kleinman, and L. E. Howarth, Phys. Rev. **126**, 1710 (1962).
[13] A. S. Barker, Jr., and J. J. Hopfield (to be published).